JOURNAL OF MATERIALS SCIENCE 18 (1983) 133–139

Study of fracture toughness evaluation of FRP

H. YANADA, H. HOMMA
Department of Energy Engineering, Toyohashi University of Technology, Toyohashi, Japan

Using the fibre reinforced plastics (FRP) laminates consisting of glass chopped strand mat and unsaturated polyester resin, experiments were conducted under various conditions in order to determine the fracture toughness for crack instability. Crack growth was judged not by cracking of the resin matrix but by break of the glass fibres. The crack front was considered to be located in the section which was cracked through the 90% of the specimen thickness. Crack extension resistance (R-curves) thus obtained did not significantly vary with specimen thickness and initial crack length, but depended greatly on specimen configurations, compact tension (CT) and centre-cracked tension (CCT) specimens. The R-curve for a CT specimen was steeper than the one for a CCT specimen, which is quite contrary to the tendency for metals. It was deduced that the instability fracture toughness calculated from the maximum load on a load–deflection diagram, K_{max}, was scarcely affected by specimen thickness, initial crack length and specimen geometry (i.e. loading configuration), and therefore could be regarded as a material constant of the FRP used.

1. Introduction

Composites, especially various kinds of fibre reinforced plastics (FRP) have been used extensively as structural materials for their excellent mechanical properties. Recently, many studies have been conducted in the framework of fracture mechanics to evaluate fracture toughness of FRP. The amount of data obtained so far, however, is not yet sufficient to establish a fracture toughness testing method for FRP. Fracture toughness is defined in different ways in the studies. Most of the definitions [1–4] are based on the initiation of stable crack growth from the same point of view as for metallic materials. The fracture toughness is expressed in terms of the stress intensity factor or the J-integral at the crack initiation, K_{Ic} or J_{Ic}. On the other hand, Garg and Trotman [5, 6] obtained fracture toughness values for crack instability by using the maximum load on the load–displacement curve and designated it maximum load toughness, K_{max}.

In general, a large amount of stable crack growth takes place prior to unstable fracture in FRP, and FRP possesses a relatively great margin in load-carrying capability even after the onset of crack extension. Therefore, the initiation toughness is an underestimate of the fracture strength of FRP.

Meanwhile, the three-dimensional finite element analyses for a through-thickness crack in a cross-plied laminate [7, 8] indicated that classical $1/r^{1/2}$ stress singularity was maintained for in-plane stresses which vary through the thickness and were discontinuous at the play interface. They indicated also that even though the crack tip zone was damaged by subcracks parallel to the fibres of each ply, the stress distribution outside the damage zone was nearly identical with that for the crack without a damage zone. Also the subcracks in that zone made the in-plane stresses at the crack tip relaxed in a similar manner to plastic deformation in metals but caused no shift in the singular stress field which would require a crack length correction. Though the FRP used in this work is different from the one employed in the above analyses and the appearance of the damage zones are also different, we may assume the $1/r^{1/2}$ singular stress field to be ahead of the crack tip.

0022–2461/83/010133–07$03.34/0

TABLE I Constituents of the FRP laminates

Glass fibre	EM600
Matrix	UP
Glass content (wt %)	33

Therefore, unless the material used has inherent nonlinearity in the constitutive equation, and as long as the damage zone ahead of the crack tip is small compared with the crack length, linear elastic fracture mechanics can be applied to the fracture of FRP even if stable crack growth occurs prior to unstable crack propagation.

The above discussion makes us pay much attention to unstable crack propagation. The crack instability toughness values are obtained for various dimensions of the specimen, and the effects of specimen thickness, initial crack length, and specimen geometry (i.e. type of loading) on the toughness are examined. From the results obtained, it is discussed whether K_{max} was a material constant of the FRP used in the experiments.

2. Experimental procedure

2.1. Materials

The FRP used in this experimental programme was composed of 600 g m^{-2} E-glass chopped strand mat (EM600) and unsaturated polyester resin (UP) as shown in Table I. The glass content was 33 wt%. Laminates were made of 4 to 20 plies according to the aims. Thickness of the layer ranged from 1.10 to 1.25 mm. Lamination of 3 to 5 plies was made at once and it was repeated every 3 to 4 h until the laminates were thickened to given values. The laminates were left for one day, and then post-cured at 100° C for 3 h in a temperature-controlled oven. The dimensions of the laminates were 400 mm x 400 mm and were so large that 25 compact tension specimens (CT) or 4 centre-cracked tension specimens (CCT) could be machined out from one laminate.

It may be presumed that chopped strand mat is macroscopically isotropic in plane and that the stress components in the laminates are constant through the thickness when they are subjected to in-plane loading since each layer of the laminate consists of the same constituents. Moreover, this kind of laminate does not show nonlinearity on the load–displacement curve as long as debonding between fibres and resin or cracking does not take place. Therefore, the linear elastic fracture mechanics approach is applicable to the fracture behaviour of laminates.

2.2. Specimen configurations and dimensions

Two kinds of specimens used are shown in Fig. 1. In order to examine the effect of specimen thick-

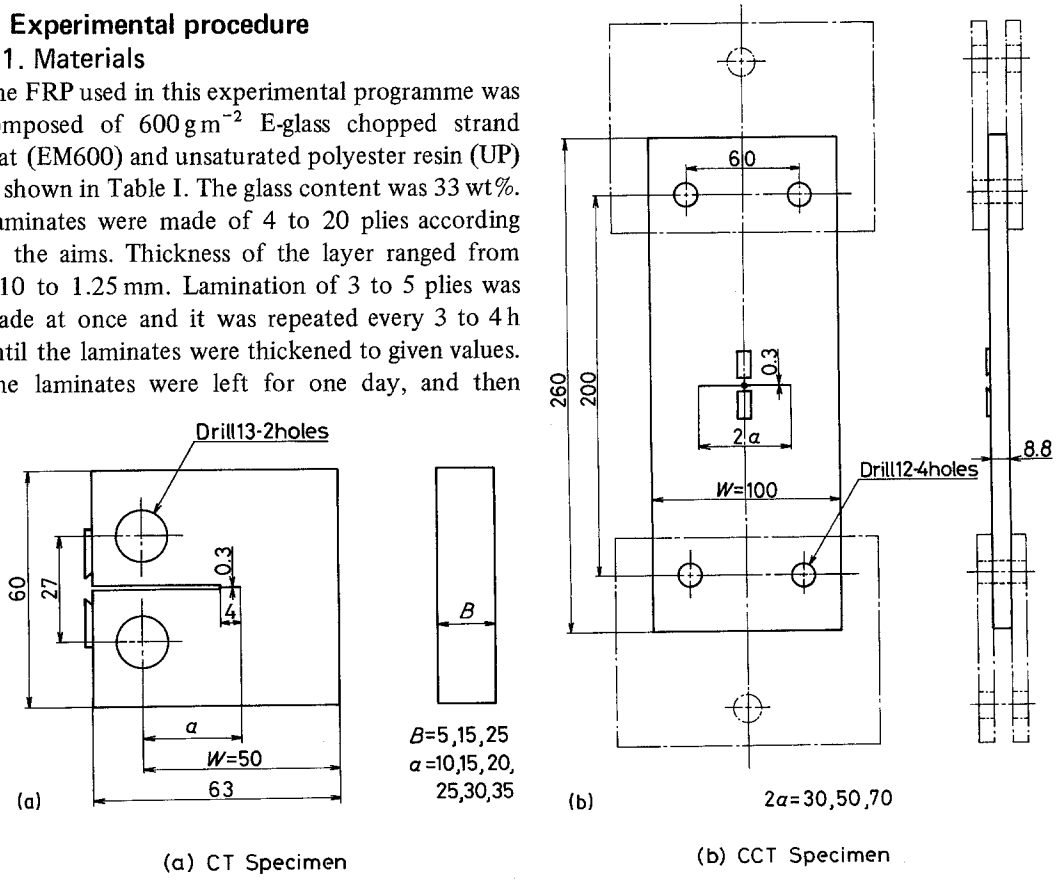

(a) CT Specimen (b) CCT Specimen

Figure 1 Specimen configurations and dimensions. (a) CT specimen and (b) CCT specimen.

ness on fracture toughness, CT specimens with different thickness values of 5 mm (4 plies), 15 mm (12 plies) and 25 mm (20 plies) were prepared, where the initial crack length was fixed to $a/W = 0.5$ (where W is the specimen width and a is the crack length). Dependency of fracture toughness on initial crack length was investigated by using CT specimens with a thickness of 15 mm. Initial crack length was varied with values of $a/W = 0.2$, 0.3, 0.4, 0.5, 0.6 and 0.7. Since it is difficult to detect a fatigue crack front in FRP, a 0.3 mm wide saw cut was introduced at the bottom of a 1 mm wide notch machined by a grinding cutter. Experiments using CCT specimens were also conducted to examine the effect of loading configuration on fracture toughness. The thickness of the CCT specimens was about 8.8 mm (7 plies), and the initial cracks were lengthened to $2a/W = 0.3$, 0.5 and 0.7, from a 2 mm diameter hole drilled at the centre of the specimen by means of 0.3 mm wide saw.

2.3. Experimental details

Two knife edges were fixed by screws crossing the crack mouth on the side surface of a CT specimen or in the middle of a CCT specimen as shown in Fig. 1. Then a clip-on gauge was mounted on the knife edges. After that, a specimen was loaded at an increasing rate of $1.09\,\mathrm{MN\,m^{-3/2}\,sec^{-1}}$ stress intensity by means of a closed-loop-type hydraulic servo material testing machine. The load, P, and the crack opening displacement, δ, were recorded by an X–Y recorder.

In fracture toughness tests, it is important to detect initiation of crack growth and crack extension values. However, this is more difficult to detect in FRP than in metallic materials because even if cracking takes place in the matrix of FRP, fibres may not be broken. Here, initiation of crack growth was defined as the fracture of fibres at the crack tip because even though the matrix ahead of the crack tip is cracked, the unbroken fibres at the crack tip possess a large load-carrying capacity. Also the crack extension was measured according to the definition of the crack tip based on the fracture of the fibres. Several techniques are utilized for the detection of crack extension. Examples include ultra-sonic wave, acoustic emission, ink-permeation into the crack tip and change in compliance of the specimen with crack growth. However, it seems that it is difficult to distinguish between cracking in the matrix and the fracture of fibres using the above techniques.

In this experiment, specimens were loaded up to certain levels of stress intensity, K_R, and then unloaded. Ligament sections including the initial crack tip were cut off from the specimens and the pieces were abraded little by little from the initial crack tip side to the section where 90% of the specimen thickness was cracked. The total depth removed was measured to obtain the crack growth value. Initially the crack growth takes place near the midsection of the specimen thickness. The amount of crack growth at the surface of the specimen is small in comparison with that at the inner region. The strength of the local portion in a specimen is scattered due to the nonuniform distribution of the fibres in the specimen. Consequently, zones where the crack propagation is strongly obstructed may exist in the specimen. Therefore, the tip of a stable growing crack was defined by the 90% cracking of the specimen thickness.

The stress intensity factor, K, was calculated by use of the following expressions.

For CT specimens [9],

$$K = (P/BW^{1/2})f(a/W) \quad (1)$$

$$f(a/W) = (2 + a/W)(0.886 + 4.64a/W - 13.32a^2/W^2 + 14.72a^3/W^3 - 5.64a^4/W^4)/(1-a/W)^{3/2} \quad (2)$$

For CCT specimens [10],

$$K = (P/BW)(\pi a)^{1/2} f(2a/W) \quad (3)$$

$$f(2a/W) = [1 - 0.025(2a/W)^2 + 0.06(2a/W)^4]\,[\sec(\pi a/W)]^{1/2} \quad (4)$$

where P is the applied load and B is the specimen thickness. The crack extension resistance, K_R, was calculated using the physical crack size, that is, the total of the original crack size and crack extension.

3. Results

3.1. Load–displacement (P–δ) curve

Typical load–crack opening displacement (P–δ) curves are shown in Fig. 2. The result in Fig. 2a is a P–δ curve for a 15 mm thick CT specimen with an initial crack length of $a/W = 0.5$ and that in Fig. 2b is a P–δ curve for a CCT specimen with an initial crack length of $2a/W = 0.5$. In the case of a CT specimen, the curve deviates from linearity above 1.6 kN, whereas in the case of a CCT speci-

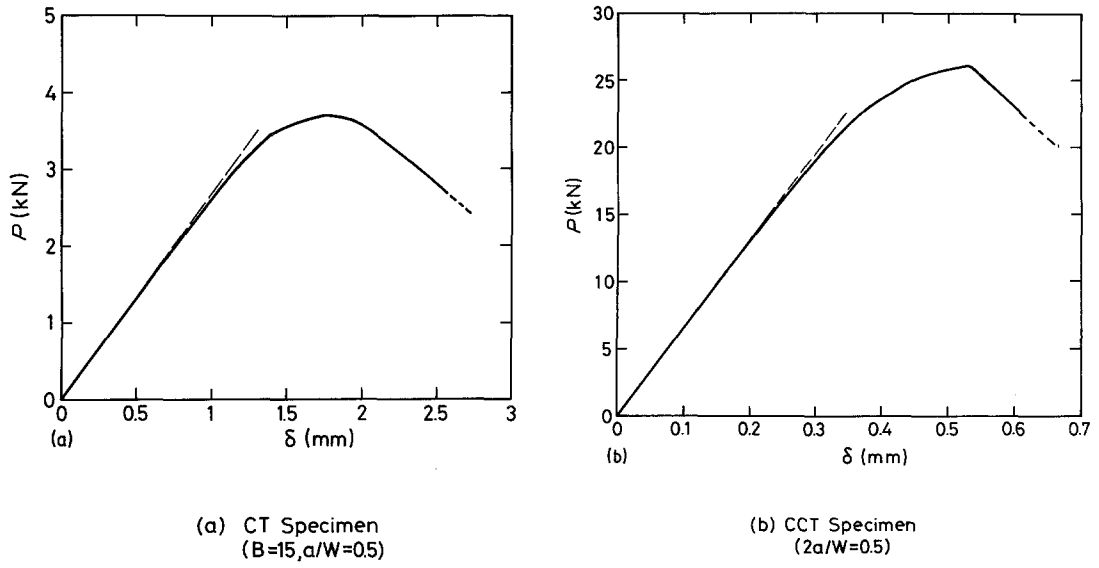

Figure 2 P–δ curves. (a) CT specimen ($B = 15$, $a/W = 0.5$) and (b) CCT specimen ($2a/W = 0.5$).

men, the linearity is lost beyond 11 kN. However, the ratio of the load to the maximum load is about 43% in each case.

3.2. Effect of specimen thickness on crack instability toughness, K_{max}

The three R-curves shown in Fig. 3 are for CT specimens with three different thicknesses. Each point in Fig. 3 was obtained from one specimen. Though the results are scattered in a relatively wide band, the R-curves obtained by the least square method for $B = 15$ mm and $B = 25$ mm are in the 95% confidence band for $B = 5$ mm and the three R-curves are almost identical. Therefore, it can be deduced that the R-curve is independent of specimen thickness. In Fig. 4 the instability toughness, K_{max}, and the initiation toughness, K_i, are plotted against the thickness. The fracture toughness for the onset of crack growth, K_i, is independent of the specimen thickness and the value is 3.6 MN m$^{-3/2}$. The fracture toughness values at the crack instability, K_{max}, are within the 8% scatter band around the mean value of 12.6 MN m$^{-3/2}$ for a specimen thickness of 5 to 25 mm. The toughness, K_{max}, can also be regarded as an independent value of the specimen thickness. The value of K_{max} is about four times the value of K_i. Therefore, it should be noticed that the FRP used in this work still possesses a considerable margin for load-carrying capability after the onset of crack growth. The crack length at the moment

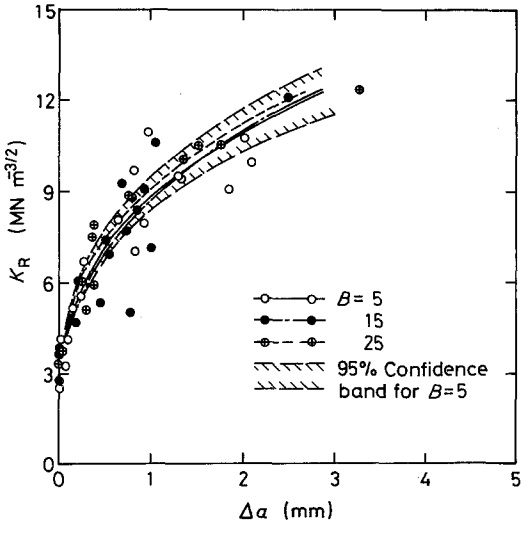

Figure 3 R-curves for different thickness of CT specimen.

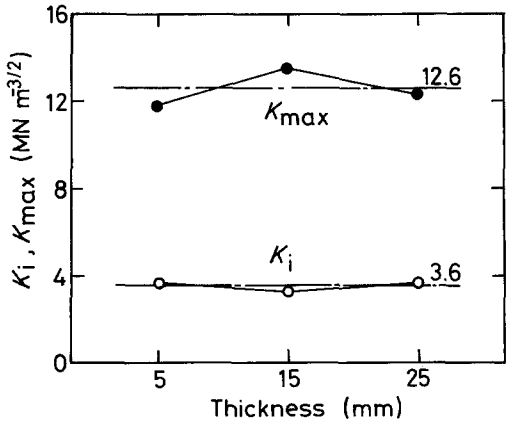

Figure 4 Thickness effect on K_{max}.

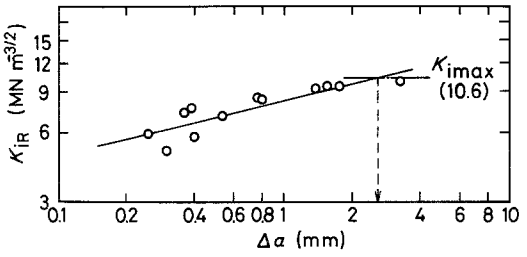

Figure 5 K_{iR}–Δa curve for CT specimen of thickness 25 mm.

of crack instability was required to calculate K_{max}, but this cannot be measured on the fracture surface since there are no distinguishing features left between the regions of the stable crack growth and that of the unstable one. So the crack extension, Δa, was plotted as a function of the stress intensity factor, K_{iR}, calculated using the original crack length on a logarithmic diagram. The K_{iR}–Δa curve for a specimen thickness of 25 mm is shown in Fig. 5. Their relationship can be expressed to a relatively good approximation by the following equations obtained by the least square method as indicated by Garg and Trotman [5, 6].

$$K_{iR} = A(\Delta a)^{\beta} \quad (5)$$

$$K_R = A'(\Delta a)^{\beta'} \quad (6)$$

where A, A', β and β' are constants. The critical value of the stable crack extension was given by the substitution of K_{imax}, calculated using the maximum load obtained from the load–deflection diagram, into Equation 5. Five specimens were used to obtain K_{max} for each specimen thickness.

3.3. Effect of the initial crack length on K_{max}

The R-curves for six different sizes of initial crack length are shown in Fig. 6. The R-curves obtained by the least square method for a/W of 0.3 and 0.7 are steeper than the other ones, but all R-curves are in the 95% confidence band of the one for $a/W = 0.5$. Therefore, the R-curves can be considered to be independent of the initial crack length. In Fig. 7 the K_{max} and the K_i values are plotted against the initial crack length. It can be seen from Fig. 7 that the values of K_{max} and K_i do not vary remarkably with the original crack length and they can be considered to be constant regardless of the initial crack length.

3.4. Effect of the type of loading on K_{max}

Three R-curves shown in Fig. 8 were obtained for three sizes of initial crack length in CCT specimens. The R-curves coincide well with each other

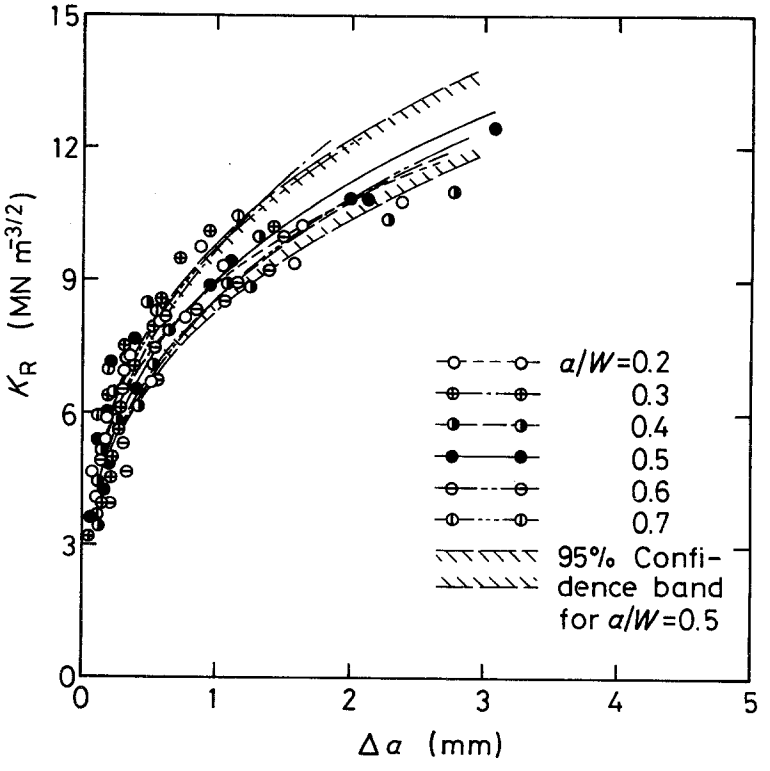

Figure 6 R-curves for various initial crack lengths of CT specimens.

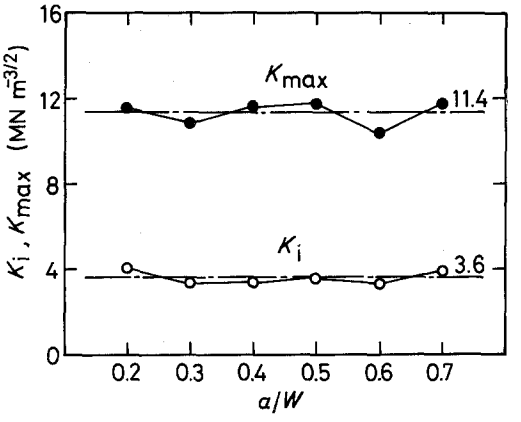

Figure 7 Effect of initial crack length on K_{max} and K_i.

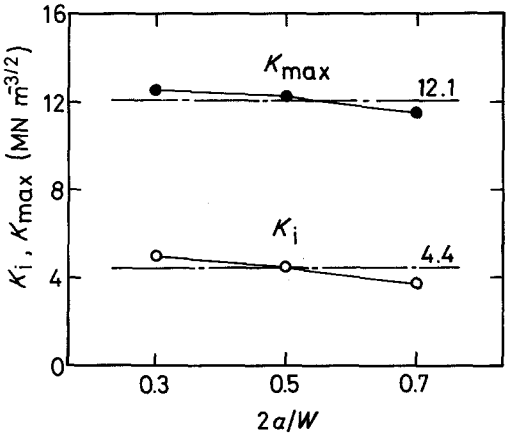

Figure 9 Effect of initial crack length on K_{max} and K_i for CCT specimens.

and they are independent of the initial crack length like those in the CT specimen, though those in the two specimen geometries are different in shape. The stable crack extension is significantly larger in CCT specimens than in CT specimens for a given resistance toughness. In Fig. 9 K_{max} and K_i are plotted against the initial crack length. It is seen that K_{max} and K_i have almost constant values for each crack length in the CCT specimen as well as in the CT specimen. As seen in Figs. 7 and 9, the value of K_{max} obtained in the CCT specimen is 10% larger than the one obtained for the CT specimen. However, the difference does not seem significant if we notice that the initiation toughness, K_i, is correspondingly larger in the CCT specimen. The difference must be caused by the scatter in the laminating process among the laminates and the antiplane bending that often occurs in the tension of a plate.

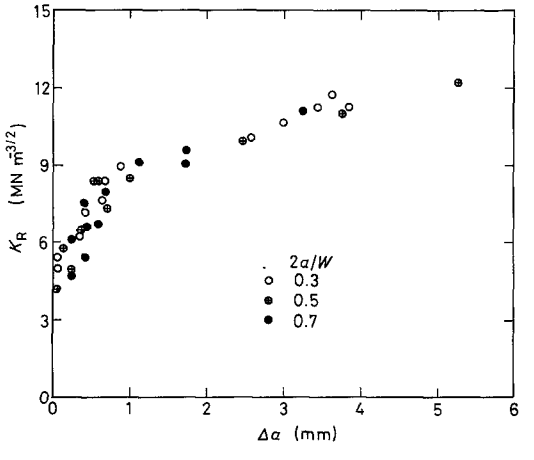

Figure 8 R-curves for different initial crack lengths of CCT specimens.

4. Discussion

As seen in Fig. 4, the fracture toughness, K_{max}, attains the maximum value for the 15 mm thick specimen. However, this is not compatible with the dependency of fracture toughness on specimen thickness. It is natural to consider that the scatter in mechanical properties among the laminates resulted mainly in the variation of K_{max} as indicated in Fig. 4. Also, this is the case for the slight variation of K_{max} with the original crack length in Fig. 7. Furthermore, the value of K_{max} for the 15 mm thick specimen in Fig. 4 and the value for the initial crack length of $a/W = 0.5$ in Fig. 7 are a little different, and their difference is as large as 14% of K_{max}, although the results are for the same thickness and the same initial crack length. In this case, it seems that the test temperature is one of the main causes of this difference in addition to the scatter in mechanical properties between the two laminates. The temperature was 18° C when the experiment on the effect of the specimen thickness was conducted, whereas another experiment was made at the temperature of 27 ± 1° C. Unlike metals, a positive correlation between the tensile strength and the fracture toughness exists for composite materials. Therefore, it can be surmised that the fracture toughness, K_{max}, became greater at the lower temperature because of an increase in tensile strength with a decrease of temperature.

Generally speaking, when stable crack extension largely occurs prior to the unstable fracture in metals, the instability fracture toughness, K_c, varies considerably with the change of loading configuration, or with the specimen thickness. For instance, K_c decreases to the plane strain

fracture toughness value and becomes independent of the specimen thickness as specimen thickness increases. The amount of stable crack growth also depends on the specimen thickness in a similar manner, and becomes negligibly small at the plane strain fracture toughness K_{Ic}. On the other hand, in the case of the FRP used in this work, K_i and K_{max} are nearly constant for 5 to 25 mm thick specimens, in spite of the existence of the few millimetres stable crack extension, as shown in Figs. 3 and 4. Also, we can see from Figs. 6 and 9 that the fracture toughness, K_{max}, is independent of the initial crack length and of the type of loading. If the initiation toughness, K_i, is adopted for a fracture criterion of the FRP, the residual strength of the components of the FRP will be extremely underestimated, and it seems inappropriate from the viewpoint of resources conservation.

From the above discussion on the instability toughness, K_{max}, we can deduce that the mechanism of stable crack growth observed in the fracture toughness tests of the FRP is essentially different from the one in metals which results from large-scale plasticity in the vicinity of the crack tip. In fact, both the constituents of the FRP used in this study, glass fibre and unsaturated polyester resin, are very brittle in their fracture behaviour.

Thus, the results obtained in the experiments show that the instability toughness, K_{max}, is constant under various conditions, that is, it is independent of specimen thickness, initial crack length and loading configuration (i.e. specimen geometry). Therefore, we may regard the instability toughness, K_{max}, as a material characteristic constant. As shown in Fig. 10, although there is a significant difference in the amount of stable crack growth between CT and CCT specimens, the values of K_{max} for both the specimens are almost equal. This fact also supports the above deduction.

Further investigation, however, will be necessary to clarify what the process of stable crack growth in FRP originates from.

5. Conclusions

For the FRP used in this work, the instability fracture toughness, K_{max}, is hardly affected by specimen thickness, initial crack length and loading configuration (i.e. specimen geometry), and is nearly constant. Therefore, the toughness, K_{max}, can be regarded as a material constant.

Further investigation is necessary to examine whether the toughness, K_{max}, is a material constant for other types of FRP, e.g. glass-roving cloth, FRP consisting of carbon fibre and epoxy resin, and so forth.

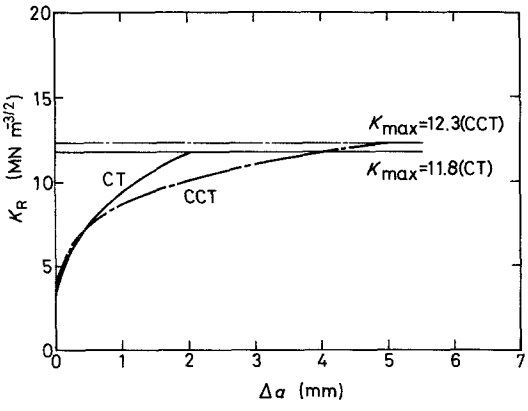

Figure 10 Comparison of R-curves for CT and CCT specimens: CT specimen with $B = 15$ mm and $a/W = 0.5$, CCT specimen with $2a/W = 0.5$.

References

1. M. ZAKO, H. MORI and T. MIYOSHI, *Trans. JSME* **45** (1979) 395, p. 726.
2. M. SUZUKI, M. IWAMOTO, Y. MURATA and K. KIRIMURA, *Trans. JSME* **47** (1981) 418, p. 603.
3. M. SUZUKI, M. IWAMOTO, K. KIRIMURA and N. TANAKA, preprint of *JSME* **810** (1981) 7, p. 183.
4. M. SUZUKI, M. NAKANISHI, M. IWAMOTO, Y. NAKAJIMA and Y. OGINO, preprint of *JSME* **810** (1981) 11, p. 56.
5. A. C. GARG and C. K. TROTMAN, Proceedings of an International Conference on Fracture Mechanics in Engineering Application, Bangalore, India, March 1979 (Sijthoff and Noord Aphen aan den Rijin, The Netherlands, 1979) p. 373.
6. A. C. GARG and C. K. TROTMAN, *Eng. Fract. Mech.* **13** (1980) 357.
7. S. S. WANG, J. F. MANDELL and F. J. McGARRY, ASTM STP 593 (1975) p. 35.
8. S. S. WANG, J. F. MANDELL and F. J. McGARRY, ASTM STP 593 (1975) p. 61.
9. "1979 Annual Book of ASTM Standards", Part 10, E399 (1979) p. 540.
10. H. TADA, *Eng. Fract. Mech.* **3** (1981) 345.

Received 22 December 1981
and accepted 23 June 1982